

Optimal Torque Control of PMSG-based Stand-Alone Wind Turbine with Energy Storage System

Mohammad Hassan Jafari Nodoushan * Mahdi Akhbari †

In this paper optimal torque control (OTC) of stand-alone variable-speed small-scale wind turbine equipped with a permanent magnet synchronous generator and a switch-mode rectifier is presented. It is shown that with OTC method in standalone configuration, power coefficient could be reached to its maximum possible value, i.e. 0.48. An appropriate control algorithm based on turbine characteristic is designed to extract maximum power from the turbine within a whole range of wind speed changes. Besides, energy storage devices (battery bank) are used to ensure continuous supplying loads and power quality. The AC loads are connected to the system via a single-phase inverter as domestic appliances. Dynamic stability of the system is also investigated to have a complete surveillance on the system operation in the conditions of hard wind speeds and maximum loads demand. The presented control method, and the other components of the system are modeled in MATLAB/SIMULINK environment. Simulation results show the good performance of the presented wind system in all case studies as well as active power balance.

Keywords: Stand-alone Wind Turbine; Permanent Magnet Synchronous Generator(PMSG); Boost Converter; Optimal Torque Control(OTC); Maximum Power Point Tracking(MPPT).

Received Nov. 2015; Revised April 2016; Accepted May 2016.

I INTRODUCTION

Recently, renewable energy electric power supplies have received a considerable attention due to the global concerns associated with the conventional generation and potential worldwide energy shortages. Among these renewable power supplies, variable speed wind turbines (WTs) can convert and deliver power in a cost-effective and reliable way [1-4].

Most recent researches in relation to wind turbines are focused on their connection to the grid either in the form of wind farms or in combination with other energy sources such as solar, geothermal, etc. While there are remote communities where connection with the power grid is too expensive or impractical and diesel generators are often the source of electricity. Under such circumstances, a locally placed small-scale stand-alone wind turbine system with permanent magnet synchronous generator is a low-cost and high efficiency solution to supply power to such customers.

Variable speed wind turbines have many advantages over fixed-speed turbines such as increased energy capture, operation at maximum power point, improved efficiency, and power quality. Besides, Synchronous generators with permanent magnets are widely used in WECS. Indeed, this technique can replace the field winding of synchronous machines and has more well-known advantages of compact size, the higher power density, the loss reduction, high reliability and good robustness [5-7].

The use of permanent magnet synchronous generator with a

switch-mode rectifier including an uncontrolled AC-DC converter (full-bridge diode rectifier) and a DC-DC converter, due to their advantages, is one of the most appropriate topology in these kinds of applications. Such advantages are: generator and power converter simplicity, low active switches, high reliability and low cost of the whole system [8, 9]. Extracting maximum power from the wind turbine is achieved by control of generator speed or torque which is performed by control of interfaced DC-DC converter. Such interfaced converters are: buck, boost, Buck-boost, etc. and several control strategies, according to their topologies, are designed and implemented in the literature [2],[3, 10, 11].

In reference [1], the control algorithm for the boost converter is based on maintaining the DC-link voltage constant. Also effective energy management of the stand-alone wind system consisting of PMSG, battery bank, dump load and etc. is presented. In the paper, battery bank is connected to the system via a bidirectional converter which needs extra control system and hence increasing the system complexity and cost. In [3], fuzzy logic control strategy is used to control two boost converters. In which, one converter is dedicated to MPPT of a variable speed PMSG wind turbine, and the second one has the objective to manage both the production and the storage of electricity for optimum performances of the system in respecting load demand. However, using two converters increases complexity and cost of the system.

Sliding mode control strategy for boost converter to extract maximum mechanical power from the wind turbine is presented in [5] and its performance has been analyzed. Also a new con-

*Electrical Engineering MS Student, shahed University, Tehran, Iran.

†Electrical Engineering assistant professor, shahed University, Tehran, Iran, Email : akhbari@shahed.ac.ir (Corresponding Author)

control method for boost converter is presented in [6] which controls PMSG speed. However, this converter control system is not able to obtain maximum power over the entire range of wind speeds. So this paper uses PI controllers which are simple and applicable for industrial automation. In this paper, a control strategy for the generator-side converter with output power maximization of a PMSG-based small-scale wind turbine is adopted. The generator-side switch-mode rectifier is controlled based on the optimal torque control (OTC) of the generator to extract maximum power from the wind. In fact the method requires only one active switching device, which is used to control and adjust the generator torque at its optimal values. It is a simple and low-cost solution for a small-scale wind turbine. In order to keep the DC-link voltage almost constant and to ensure supply demand at low wind speeds, the battery bank is used. So, active power balance in the system during whole wind speed changes is maintained as well as MPPT. In addition, by showing WT power coefficient, good system dynamic response is also presented.

This paper is organized as follows. In Section II, the stand-alone wind system configuration is presented and main parts are introduced; then, Section III describes the proposed control strategy and its algorithm. The simulation results and discussions are provided in Section IV, while conclusions are presented in Section V.

II STAND-ALONE WIND SYSTEM CONFIGURATION

A System overview

Fig. 1 shows the wind system configuration. The studied topology consists of a wind turbine with a power rating of 3.1 kW, PMSG with the nominal output power of 2-kW, a three-phase diode bridge rectifier, a boost converter, an inverter and transformer with the output rating of 230V/50 Hz, a 2-kW AC load, and a battery bank with the power rating of 2-kW. Similar stand-alone wind energy system is already being developed in [7],[6], but this paper focuses on the system operation under OTC of the generator, MPPT of the proposed strategy, and active power balance of the system within a whole range of wind speed variations.

The mechanical power captured by wind turbine is delivered to PMSG which is converted into electrical form and then transferred to loads via converters. During this process, some power is lost and as wind speed increases, these losses increase too. Overall wind power conversion system and its losses is clarified in Fig. 2 where generator losses are the main part.

B Variable speed wind turbine

The mechanical power extracted by the wind turbine is expressed as (1) [12, 13]:

$$P_m = 0.5C_p\rho A V_w^3 \quad (1)$$

The operation coefficient (C_p) of wind power turbines defined by (2) :

$$C_p = 0.22 \left(\frac{116}{\lambda_i} - 0.4\beta - 5 \right) e^{-12.5/\lambda_i} \quad (2)$$

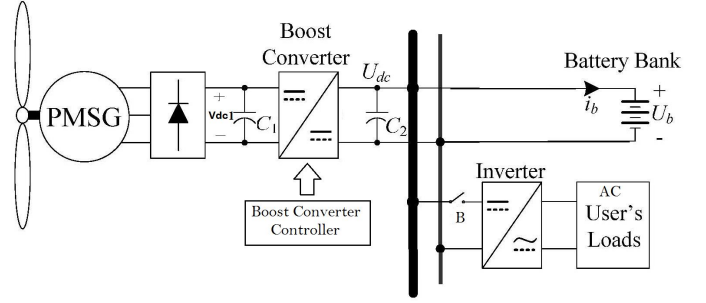


Figure 1: Wind system configuration

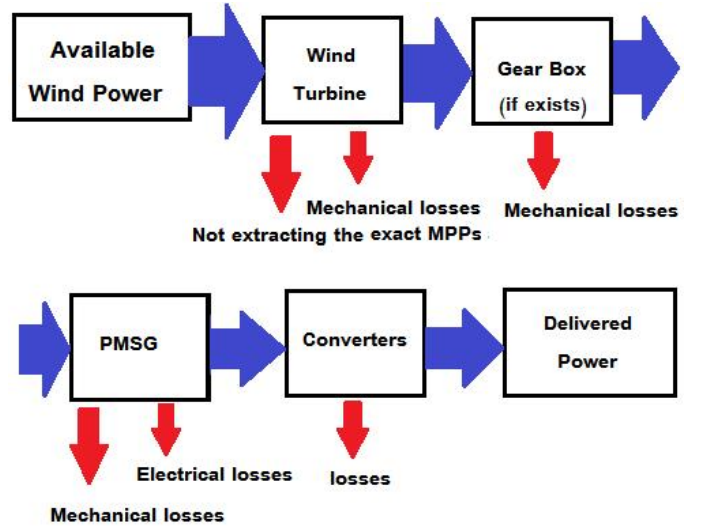


Figure 2: Losses in wind power conversion process

Small-scale wind turbines usually do not have the blade angle control mechanism so $\beta=0$. Also λ_i is a factor which is a function of the blade angle and tip speed ratio λ as determined by (3) and (4):

$$\frac{1}{\lambda_i} = \frac{1}{\lambda + 0.08\beta^2} - \frac{0.035}{\beta^3 + 1} \quad (3)$$

$$\lambda = \frac{R\omega_m}{v_w} \quad (4)$$

Wind turbine parameters studied in this paper are given in the Appendix. Fig. 3 shows wind turbine output power versus rotor speed in different values of wind speeds typically from 4 m/s to 9 m/s. It is observed that at any wind speed, there is one maximum power point (MPP) which can be extracted from WT. OTC curve is compared with MPPs curve which is further verified by simulations. As it is clear, except for very high wind speeds, OTC strategy could trace MPPs very well. Compared with the control strategy mentioned in [6], with the similar system topology, OTC could achieve higher efficiency. For the wind turbine, optimal torque points are not maximum ones [14]. As illustrated in Fig. 4, wind turbine output torque achieved by the presented strategy, is very close to its optimal values. Detailed controller performance and system behavior are simulated and discussed in section IV.

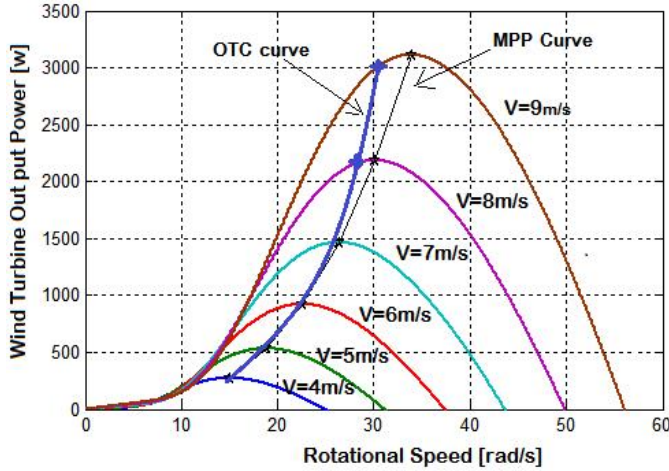


Figure 3: Wind turbine output power versus rotor speed in different values of wind velocity

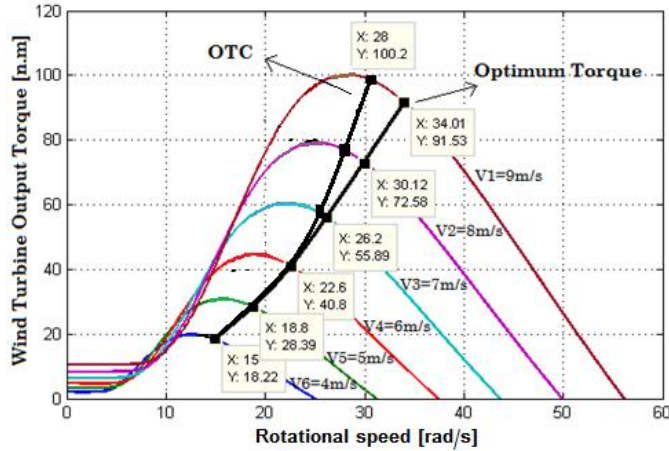


Figure 4: Wind turbine torque versus rotor speed at different wind speeds

C Energy storage system

Using a set of batteries in series or parallel to form a battery bank (BB) as an energy storage system in stand-alone WECS not only increases reliability of the system but also keeps the DC-link voltage nearly constant. In addition, it makes the fluctuations and transient states of the system smoother[15] When the wind speed is greater than the amount required to meet the consumer demand, the excess generated power is stored in BB and vice versa, when the wind speed is less than the amount required to meet the load demand, the BB discharges. So, the active power balance of the system has been established. In this paper, BB consists of ten lead-acid batteries (LABs) with nominal voltage of each one 12 volts and 26 amp-hours nominal capacity which are connected in series. Details about LAB modeling can be found in [16],[17].

To express the amount of charge or discharge of the battery, the parameter State Of Charge (*SOC*) is introduced and can be written as (5), where it is equal to the initial state of charge (*SOC*₀) of the battery plus the amount of amp-hours of power injected/extracted from it (*I*_b is the battery current). It should

be noted that all these parameters are expressed in percentage of the nominal capacity *Q*_n [6].

$$SOC_{[\%]} = SOC_{0[\%]} + \left(\frac{1}{Q_n} \int_0^t I_b dt \right) \cdot 100 \quad (5)$$

III OTC ALGORITHM

Considering the fluctuating nature of wind, and wind turbines power curve, to extract maximum power, the generator torque or speed must be adjusted proportional to the wind speed. OTC method controls the generator torque and adjusts it in optimum value in any wind speed conditions. The method is taken from [18] but here the generator efficiency is also included in control loop design to have better operation. By placement of (4) in(1), (6) is obtained:

$$P_m = 0.5\rho A C_p V_w^3 = 0.5\rho A C_p \left(\frac{\omega_m R}{\lambda} \right)^3 \quad (6)$$

For a given wind turbine characteristics, the optimal tip speed ratio is specified. As a result, optimal mechanical angular velocity of rotor according to (4) is determined as (7):

$$\omega_{m,opt} = \frac{\lambda_{opt}}{R} v_w = K_w v_w \quad (7)$$

Optimum mechanical power *P*_{*m,opt*} is calculated by (8):

$$P_{m,opt} = 0.5\rho A C_{p,opt} \left(\frac{R\omega_{m,opt}}{\lambda_{opt}} \right)^3 = K_{opt}(\omega_{m,opt})^3 \quad (8)$$

Also optimum mechanical torque is calculated as follows:

$$T_{m,opt} = K_{opt}(\omega_{m,opt})^2 \quad (9)$$

So, the OTC algorithm is established as follows:

- 1) Measure generator speed ω_g .
- 2) Calculate the reference torque T_g^* by considering generator efficiency η_g in (10):

$$T_g^* = \eta_g K_{opt}(\omega_g)^2 \quad (10)$$

- 3) This reference torque is then used to calculate the dc reference current by measuring the rectifier output voltage V_{dc1} as given by (11):

$$I_{dc1}^* = (T_g^* \cdot \omega_g) / V_{dc1} \quad (11)$$

- 4) The error between the reference dc current and measured dc current is used to vary the duty cycle of the switch to regulate the output of the switch-mode rectifier and the generator torque through a proportionalintegral (PI) controller.

IV SIMULATION RESULTS AND DISCUSSION

The proposed system has been modeled and simulated in MATLAB/SIMULINK environment. Simulation results validate the correctness of controller performance as well as active power balance.

A System operation

Fig. 5 shows the block diagrams for simulation. In order to investigate the system performance within the whole range of wind velocities, the wind profile is considered to be like Fig. 6 in which the wind speed varies from 9 m/s as base wind to 4 m/s as Cut-out wind speed. Although it could be considered increasing, which there is no difference. Simulation results for the random wind speed variations are presented in the flowing section and dynamic response of the system is investigated. Simulations are performed for 12 seconds.

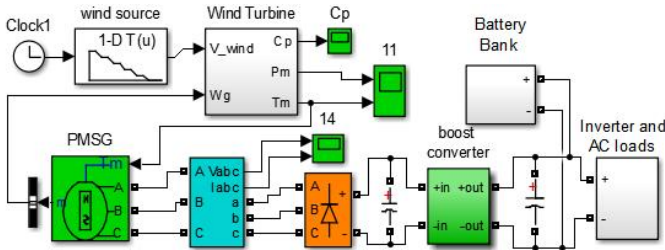


Figure 5: Simulink implementation of wind system

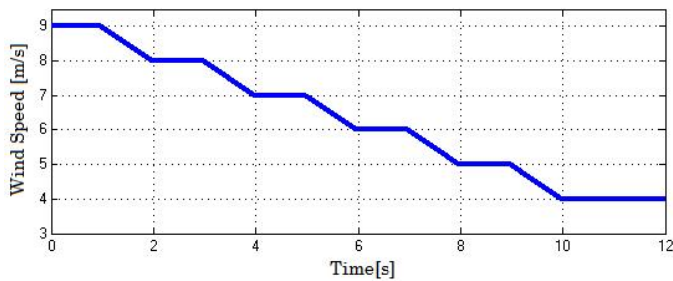


Figure 6: Wind speed profile

Fig. 7 shows different power forms of the system including WT optimum mechanical power, WT actual mechanical power, and PMSG's electrical output power. To obtain optimum power curve of the WT at different wind speed, a look-up table based on the turbine characteristic is written. So, by tracing this curve through controlling the PMSG torque, MPPT is achieved. From the figure, by comparing WT optimum and actual power curves, it is obvious that except for very high wind speed (near 9m/s) due to the major effect of diode commutation, controller is able to trace maximum power points very well [19].

Electrical output power of the PMSG is also accordance with the wind speed and hence, turbine output power. In the maximum wind speed of 9m/s, and WT out power of 3-kW, PMSG output power is about 2-kW. This difference is obviously because of the PMSG losses in form of mechanical (fraction losses) and electrical (RI^2) which were expected according to calculations. Therefore, the efficiency of %67 is obtained. But, as the wind speed decreases, PMSG output current (and voltage) decreases, resulting to achieve higher efficiency so that at low wind speed of 4m/s the efficiency reaches to more than %95.

Fig. 8 illustrates different torques in the system where optimal, actual, and PMSG reference torques are compared. Tracing the WT optimal torque by the controller is obvious but as can be

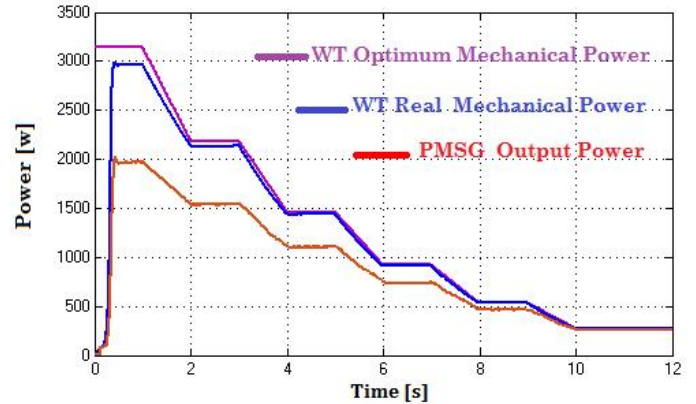


Figure 7: Power in the system

seen, just there is a little difference between them and as wind speed decreases, this difference becomes less. For example, at wind speed of 9 m/s, actual WT torque is 100 N.m, which is near to its maximum possible value, while the optimal value is 93 N.m. Thus OTC strategy leads to applying higher torque to the wind turbine. The PMSG reference torque is considered to be %70 in order to have the most proper controller operation. In fact, this torque is designed for the controller in OTC loop and its difference to other torques is not important. Since in practice WT and PMSG are directly connected to each other and experience the same torque.

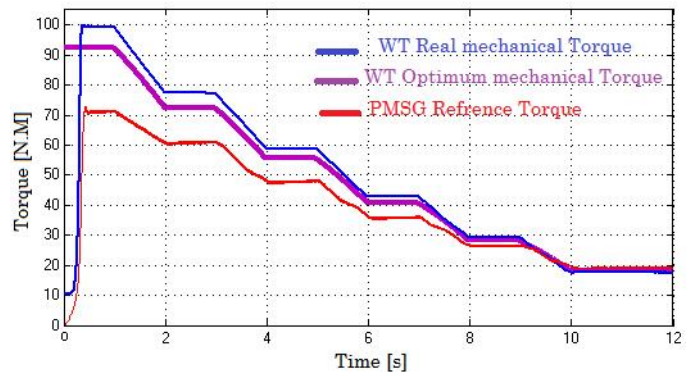


Figure 8: Wind turbine and generator torques

WT optimum rotational speed and actual rotational speed are shown in Fig. 9 where a little difference between them is clear. Unlike optimum torque, here, optimum speed is more than actual values in a wide range of wind speed variations. As a result, WT actual power is very close to its optimum values ($P=T^*$) and that, the MPPT is achieved successfully.

Three phase instantaneous voltage and current of the PMSG is depicted in Fig. 10 and Fig. 11 which are accordance with the WT speed and power. The use of SMR as a generator side converter, besides its benefits, employs harmonics to the generator voltage and current waveforms and therefore, causing torque ripples [20, 21]. This point is shown in Fig. 12.

The generator RMS and rectified voltages are shown in Fig. 13. In the nominal condition of wind speed of 9 m/s and no load

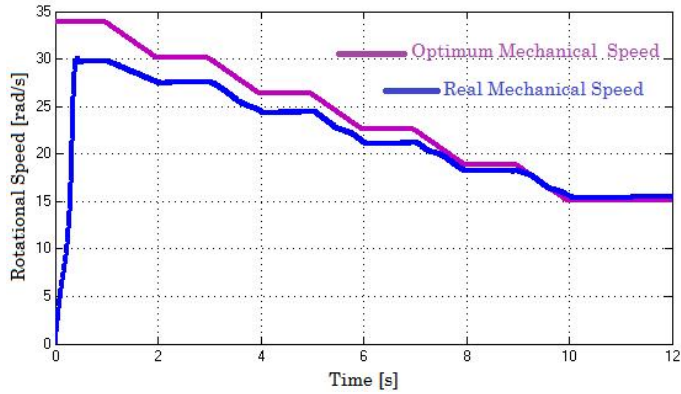


Figure 9: Optimal and actual rotational speed

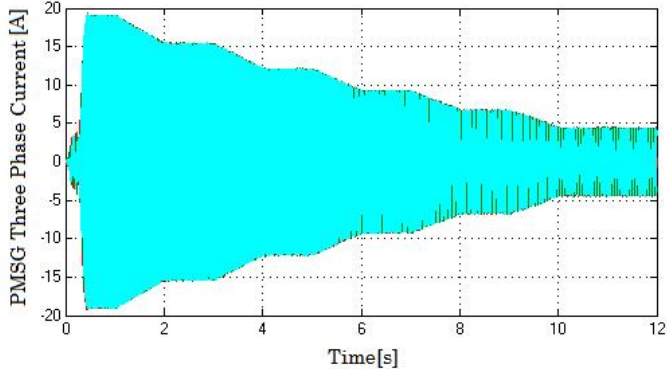
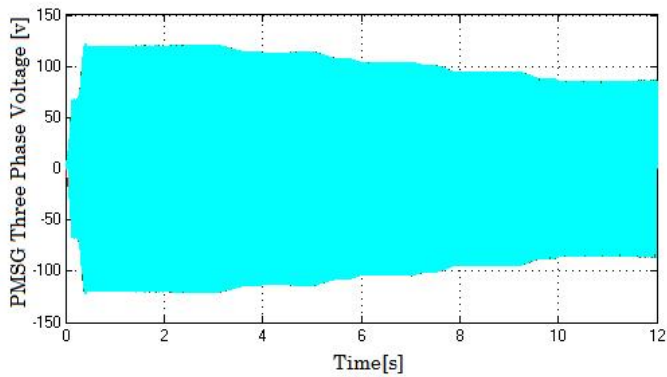


Figure 10: PMSG three phase voltage and current

connected, rectified voltage is about 120 v and rectified current is 16.7 amps (see Fig. 14). When a 2-kW load is connected, DC-link voltage and therefore, rectified voltage decreases by about 4 volts. Currents in the system are shown in Fig. 14 where, boost converter input current is always greater than the output current due to the performance of such a converter. As wind speed decreases, these currents decrease as well as generator RMS current which has a noticeable distance from those DC currents especially in high wind speed. But, in low wind speed e.g. less than 6 m/s, the generator RMS current goes higher than the boost converter output current but in any conditions they are less than the rectified DC current as it is obvious in the picture and proved by calculations.

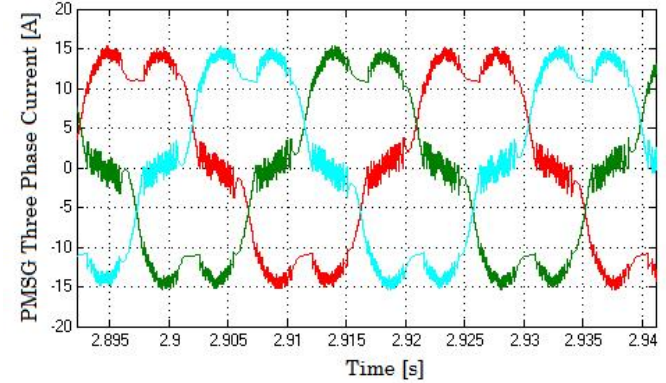
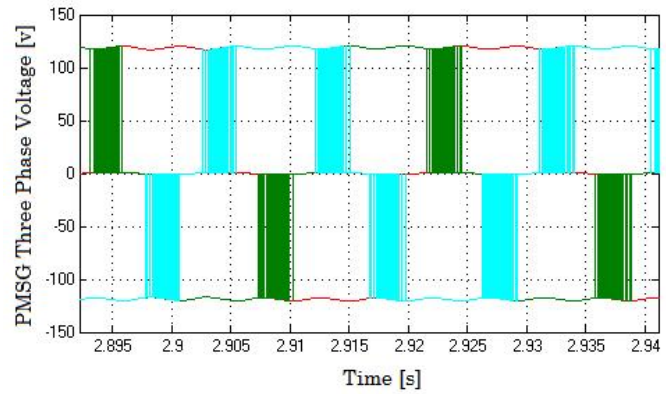


Figure 11: Instantaneous PMSG voltage and current

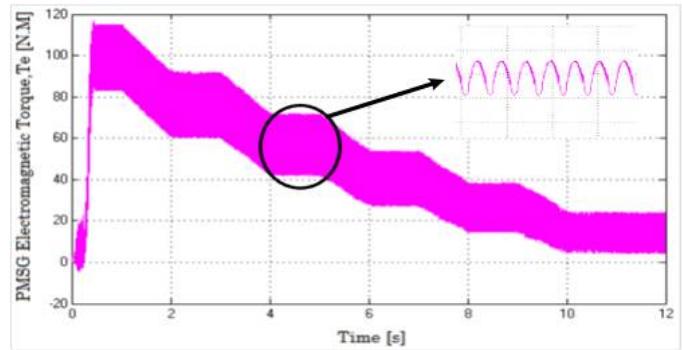


Figure 12: PMSG electromagnetic torque and its ripples

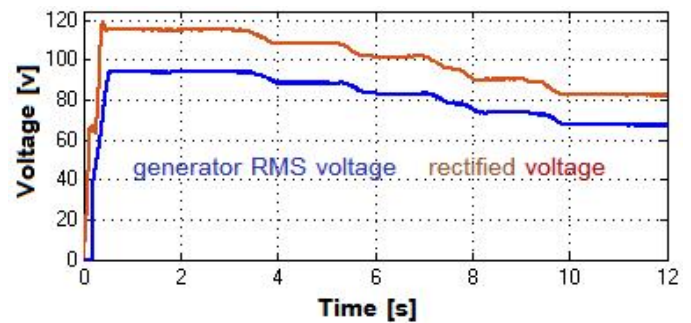


Figure 13: Generator RMS and rectified voltage

B Active power balance in the system

Fig. 15 (a) shows battery bank state of charge while its initial value (%SOC) is considered to be %75. Since a 1-kW load is

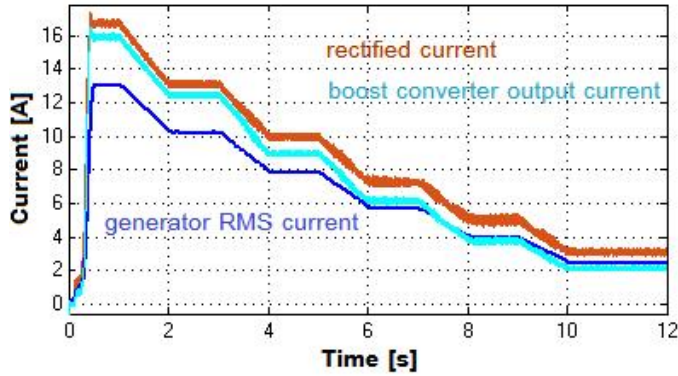


Figure 14: Different currents in the system

connected, till about $t = 5$ s the wind power generation is more than the load demand. So, the surplus power is stored to the BB and therefor, battery bank SOC increases. After that, by wind speed reduction, wind power generation cannot supply the entire load demand. As a result, BB discharges and the stored power released to ensure continuous supply of the load.

Fig. 15 (b) clearly shows active power balance of the system. In fact, wind turbine and BB are matched with each other so that a fixed load demand be supplied. For example, at wind speed of 9 m/s, the generated power by WT is 2-kW. Since the consumer load is 1-kW, the excess power charges BB and then switch to discharging mode when low wind speeds.

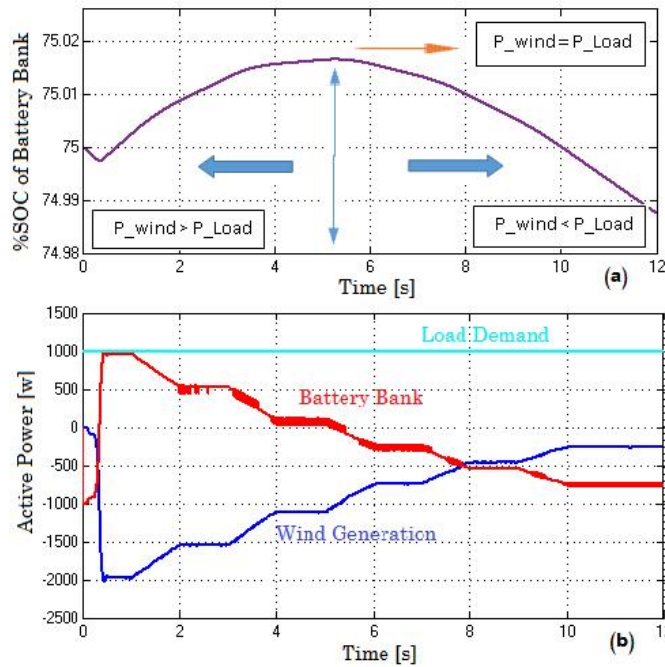


Figure 15: Active power balance in the system: %SOC of battery bank (a), continuous load supplying (b)

Fig. 16(a) shows BB current which has positive and negative values as it is expected. Also, DC-link voltage variations is illustrated in Fig. 16(b) where its nominal value is 120 volts with the maximum allowable variation of volts. Depending on the

system conditions such as wind speeds, battery bank %SOC, and the load demand, it can be more or less than this value. As it is observed from Fig. 16(b) when BB is charging, DC-link voltage increases about 3 volts and then decreases by the wind speed decreases and load demand is fixed.

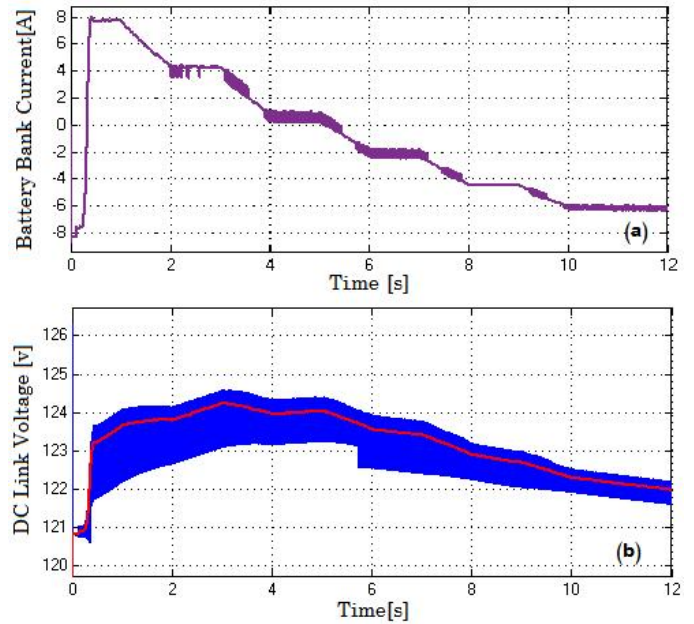


Figure 16: Battery bank values: Current (a), DC-link voltage variations (b)

C MPPT evaluation

Maximum power tracking of the presented wind turbine is achieved when operation coefficient is maintained at 0.48 which is maximum allowable value. So, keeping this coefficient at 0.48, means that MPPT is performed within the whole range of wind speed variations. Fig. 17 shows WT operation coefficient which is near 0.46 in very high wind speed and exactly 0.48 in the condition of middle and low wind speeds. So, OTC strategy by controlling and adjusting PMSG and wind turbine torque at its optimum values, can perform maximum power point tracking successfully.

Duty cycle variation is depicted in Fig. 18 where it varies from 0.03 to 0.3 at wind speed of 9 m/s and 4 m/s consecutively. Clearly, by wind speed reduction, it must increase in order to boost the voltage, control the generator and wind turbine torque, and consequently MPPT be done persuasively.

To investigate the system dynamic stability and controller performance, wind speed profile is supposed to be like Fig. 19, which consists of three steps in wind velocity at times 1, 2 and 3s consecutively. Simulations are performed for 4 seconds, and results are summarized from Fig. 20 to Fig. 22. The 2-kW AC load is connected and load demand is maximum. Fig. 20 illustrates optimum and actual wind turbine and PMSG power. It is observed that not only dynamic stability of the system is maintained, but maximum power tracking is also achieved. Wind turbine can trace optimum values very soon while the generator traces smoother and with a little delay due to its inertia [21].

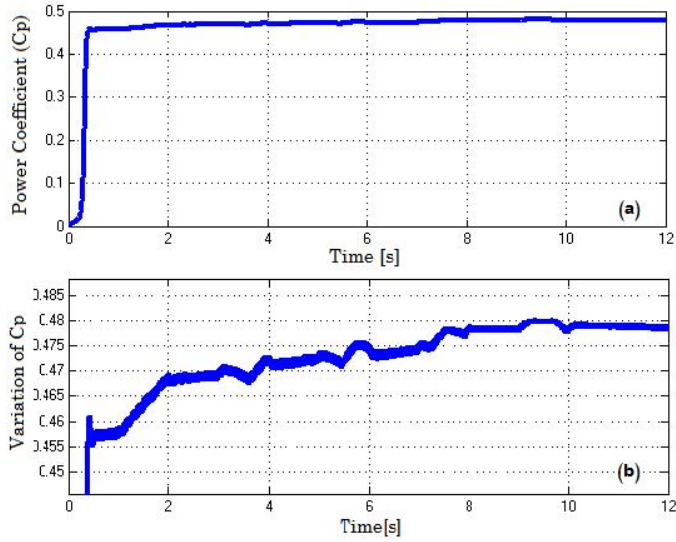


Figure 17: Wind turbine Operation coefficient and MPPT. Power coefficient (a), variation in C_P (b)

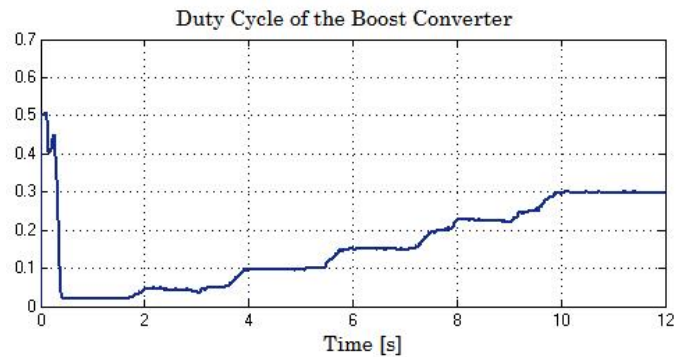


Figure 18: Boost converter duty cycle variations

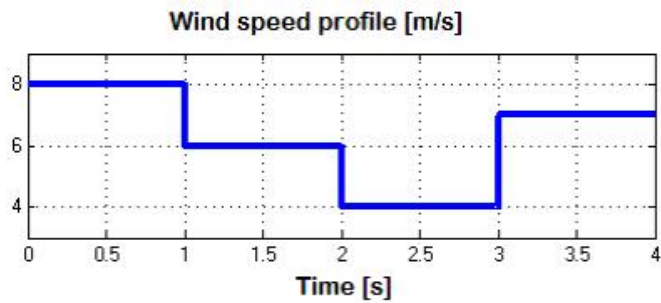


Figure 19: Wind speed variations

D System dynamic stability

Controller performance on turbine and generator torque is shown in Fig. 21. When wind speed steps down, turbine torque steps down too, but after passing transient states, it increases and then settles down to a new and stable point. It is noteworthy that controller reference torque which is used to adjust generator torque, has a lower dynamic than reference and actual ones. Operation coefficient (C_P) in Fig. 22 gives a total view of wind system response and controller operation when suffering from

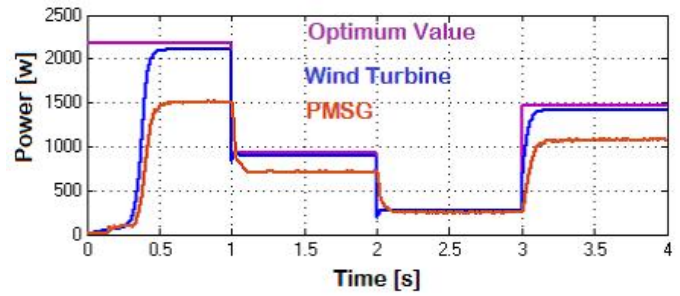


Figure 20: Tracing optimum power and dynamic response of the system and controller

high wind speed changes and maximum load demand. Wind turbine is so controlled that even in worst condition of wind speeds, operation coefficient is kept near its maximum value of 0.48 and good dynamic stability is gained.

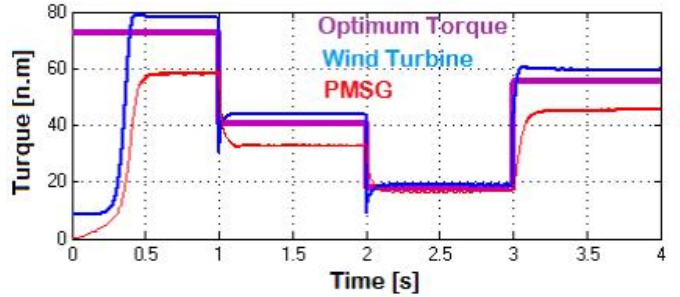


Figure 21: Tracing optimum torque and dynamic response of the system and controller

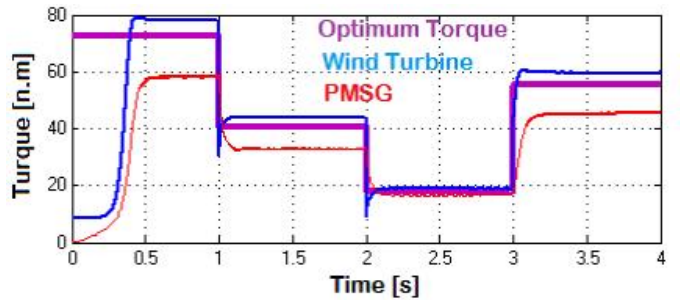


Figure 22: Wind turbine operation coefficient

V CONCLUSION

In this paper, optimal torque control of PMSG-based small-scale wind energy conversion system was investigated. This control strategy was applied to switch-mode rectifier consisting of a three phase passive rectifier and a boost power converter as an interfaced converter. By adjusting the duty cycle of the boost converter and therefore controlling generator torque to its optimum values, maximum power is extracted from the turbine within a whole range wind speed variations. To meet the maximum consumer demand in all conditions, a 260Ah battery bank was used. The storage devices are so designed to ensure the

safe supply of the loads, regardless of the problems caused by wind speeds or load variations. By simulating the presented wind system in MATLAB/SIMULINK, and analyzing the results, the good performance of the controller and battery bank is validated. Furthermore operation coefficient C_p maintained nearly 0.48 which means in all conditions of wind variations, the MPPT is achieved successfully.

VI APPENDIX

Wind Turbine Parameters :

$$P_{T_max} = 3.1kW$$

$$\rho = 1.225kg/m^3$$

$$C_{P_max} = 0.48$$

PMSG Parameters:

$$P_{in_rated} = 3kW$$

$$P_{out_rated} = 2kW$$

$$T_{m_rated} = 100N.m$$

$$\omega_{m_rated} = 30rad/s$$

$$Rated_Voltage = 120V$$

$$Rated_Current = 17A$$

$$R_s = 2\Omega, L_d = L_q = .001H$$

$$\psi_{PM} = 0.46Wb$$

$$Pole - Pairs = 8$$

REFERENCES

- [1] C. Bhende, S. Mishra, and S. G. Malla , "Permanent magnet synchronous generator-based standalone wind energy supply system," ,IEEE Transactions on Sustainable Energy, vol. 2, pp. 361-373, 2011.
- [2] H. Wang, C. Nayar, J. Su, and M. Ding, "Control and interfacing of a grid-connected small-scale wind turbine generator," ,IEEE Transactions on Energy Conversion, vol. 26, pp. 428-434, 2011.
- [3] H. Q. Minh, F. Nollet, "Control of permanent magnet synchronous generator wind turbine for stand-alone system using fuzzy logic," ,in EUSFLAT Conf., 2011, pp. 720-727.
- [4] B. Wu, Y. Lang, N. Zargari, and S. Kouro , "Power conversion and control of wind energy systems," ,John Wiley & Sons, 2011.
- [5] P. DAI, W. SHI, and J. CHEN, "A study for low-cost small power wind turbine systems," <http://www.paper.edu.cn>, pp. 36-44, 2013.
- [6] L. Barote, C. Marinescu, and M. N. Cirstea , "Control structure for single-phase stand-alone wind-based energy sources," ,IEEE Transactions on Industrial Electronics, vol. 60, pp. 764-772, 2013.
- [7] L. Barote and C. Marinescu , "PMSG wind turbine system for residential applications," ,International Symposium on Power Electronics Electrical Drives Automation and Motion (SPEEDAM), 2010, pp. 772-777.
- [8] H. Polinder, J. A. Ferreira, B. B. Jensen, A. B. Abrahamsen, K. Atallah, and R. A. McMahon , "Trends in wind turbine generator systems," ,IEEE Journal of Emerging and Selected Topics in Power Electronics, vol. 1, pp. 174-185, 2013.
- [9] R. S. Semken, M. Polikarpova, P. Rytte, J. Alexandrova, J. Pyrhnen, J. Nerg, et al., "Direct-drive permanent magnet generators for high-power wind turbines: benefits and limiting factors," ,IET Renewable Power Generation, vol. 6, pp. 1-8, 2012.
- [10] Z. Alnasir and M. Kazerani, "Performance comparison of standalone SCIG and PMSG-based wind energy conversion systems," ,in Electrical and Computer Engineering (CCECE), 2014 IEEE 27th Canadian Conference on, 2014, pp. 1-8.
- [11] Bhende, C. N., Mishra, S. , Malla, S. G., "Permanent Magnet Synchronous Generator based stand-Alone Wind Energy Supply System ," ,IEEE Transactions on Sustainable Energy, vol. 2, No. 4 , pp. 361-373, 2011.
- [12] H. Huang, C. Mao, J. Lu, and D. Wang, "Small-signal modelling and analysis of wind turbine with direct drive permanent magnet synchronous generator connected to power grid," ,IET Renewable Power Generation, vol. 6, pp. 48-58, 2012.
- [13] M. M. Hussein, T. Senjyu, M. Orabi, M. A. Wahab, and M. M. Hamada, "Simple maximum power extraction control for permanent magnet synchronous generator based wind energy conversion system," ,Conference on Electronics, Communications and Computers (JEC-ECC), Japan-Egypt, 2012, pp. 194-199.
- [14] S. Morimoto, H. Nakayama, M. Sanada, and Y. Takeda , "Sensorless output maximization control for variable-speed wind generation system using IPMSG," , Conference Record of the Industry Applications Conference, 38th IAS Annual Meeting., 2003, pp. 1464-1471.
- [15] S. W. Mohod and M. V. Aware , "Micro wind power generator with battery energy storage for critical load," ,IEEE Systems Journal, vol. 6, pp. 118-125, 2012.
- [16] O. Tremblay and L.-A. Dessaint , "Experimental validation of a battery dynamic model for EV applications," ,World Electric Vehicle Journal, vol. 3, pp. 1-10, 2009.
- [17] M. Georgescu, L. Barote, C. Marinescu, and L. Clotea , "Smart electrical energy storage system for small power wind turbines," ,12th International Conference on Optimization of Electrical and Electronic Equipment (OPTIM), 2010, pp. 1192-1197.
- [18] M. E. Haque, M. Negnevitsky, and K. M. Muttaqi , "A novel control strategy for a variable speed wind turbine with a permanent magnet synchronous generator," ,IEEE Industry Applications Society Annual Meeting, IAS'08., 2008, pp. 1-8.
- [19] N. Orlando, M. Liserre, R. Mastromauro, and A. Dell Aquila , "A survey of control issues in PMSG-based small wind-turbine systems," ,IEEE Transactions on Industrial Informatics, Volume: 9, Issue: 3, pp. 1211 - 1221 ,Aug. 2013.
- [20] Y. Xia, J. Fletcher, S. Finney, K. Ahmed, and B. Williams, "Torque ripple analysis and reduction for wind energy conversion systems using uncontrolled rectifier and boost converter," ,IET renewable power generation, vol. 5, pp. 377-386, 2011.
- [21] J. Chen and C. Gong , "On Optimizing the Transient Load of Variable-Speed Wind Energy Conversion System During the MPP Tracking Process," ,IEEE Transactions On Industrial Electronics, Vol. 61, NO. 9,2014.